Fall 12-16-2022

BIO-BASED UV-CURABLE FILMS AND THE EFFECT OF BIO-CONTENT ON THE PROPERTIES OF THE FILMS

SAHILKUMAR CHAUDHARY
Pittsburg State University, sachaudhary@gus.pittstate.edu

Recommended Citation

CHAUDHARY, SAHILKUMAR, "BIO-BASED UV-CURABLE FILMS AND THE EFFECT OF BIO-CONTENT ON THE PROPERTIES OF THE FILMS" (2022). *Electronic Theses & Dissertations*. 400.
https://digitalcommons.pittstate.edu/etd/400

BIO-BASED UV-CURABLE FILMS AND THE EFFECT OF BIO-CONTENT ON THE PROPERTIES OF THE FILMS

A Thesis Submitted to the Graduate School
in Partial Fulfillment of the Requirements
For the Degree of
Master of Science

Sahilkumar Ashvinkumar Chaudhary

Pittsburg State University

Pittsburg, Kansas

December, 2022

BIO-BASED UV-CURABLE FILMS AND THE EFFECT OF BIO-CONTENT ON THE PROPERTIES OF THE FILMS

Sahilkumar Ashvinkumar Chaudhary

APPROVED:

Thesis Advisor ____
Dr. Ram Gupta, Department of Chemistry

Committee Member ____
Dr. Charles Neef, Department of Chemistry

Committee Member ____
Dr. Timothy Dawsey, National Institute for Materials Advancement

Committee Member ____
Dr. John Franklin, Department of English and Modern Languages

Acknowledgments

I would like to express my gratitude to Dr. Ram Gupta for being a generous mentor who has fueled my passion for the research and development field. While working with him, I developed analytical expertise and an understanding of the real-life application of science. Additionally, I carried out various projects that have expanded my knowledge in different research areas. This has helped to enhance my critical thinking ability. His endless assistance during my studies at Pittsburg State University is truly honorable. His guidance has made me perceive my life more positively. I am looking forward to applying everything I learned from his hard work, discipline, and inspirational behavior to my work ethic.

I appreciate Dr. Khamis Siam, Dr. Tim Dawsey, Dr. Jody Neef, and Dr. John Franklin for their contribution to my thesis defense, and for being part of the committee. I am grateful to Dr. Peter Dvornic, Mr. Paul Herring, and Dr. Jeanne Norton for teaching me and helping me complete my Master's Degree in Polymer Chemistry. I appreciate the Department of Chemistry for giving me the scholarship to study at Pittsburg State University (PSU). I would also like to thank the National Institute for Materials Advancement for offering me in-depth information in the field of polymer chemistry. This was a life-changing opportunity and it has helped me become more qualified in the field of research and development.

I would like to thank my father Ashvinbhai and my mother Bhikhiben for their unwavering support. They are the center of my universe and are always present in my

heart. Their inspirational counsel inspires me to be successful in all aspects of my life. Without their support, I would not have been able to come to the USA and study at PSU. Furthermore, I would like to thank my colleagues: Prashant, Choi, Tenzin, Felipe, Magdalene, Vishwa, Shiva, Arjun, Yash, Mahesh, Rishabh, Prasadi, and Teddy. They value my work, help me stay on track with my studies, and create enjoyable memories at PSU. I would also like to thank everyone who has assisted me and taught me the necessary lessons to start my new career in the United States.

BIO-BASED UV-CURABLE FILMS AND THE EFFECT OF BIO-CONTENT ON THE PROPERTIES OF THE FILMS

An Abstract of the Thesis by
Sahilkumar Ashvinkumar Chaudhary

The use of renewable resources in film formation has become a new focal point for industry because it is abundantly available and has less carbon emission during production than traditional ones. This has drawn researchers to investigate the functionality of bio-based raw materials and their end-usage. By modifying their chemical structures, the properties of these films like thermal resistance, impact resistance, and chemical resistance can be increased. In this research, limonene was used as a partial replacement for petroleum-based chemicals in film formation. A two-step chemical process was carried out to modify the limonene and the final product was used in film formulations. Titration and Fourier transform infrared spectroscopy (FTIR) analysis were used to confirm the structure of the modified limonene. The UV-cured films were also analyzed by tensile, flexural, hardness, and thermal tests to examine their mechanical and thermal properties.

Limonene oil was modified using a thiol-ene reaction to introduce hydroxyl functionality to prepare a limonene diol (LD). Then, a methacrylation reaction was carried out to synthesize methacrylated limonene diol (MaLD) with a byproduct of methacrylic acid and this mixture is referred to as ML-Ma. To prepare a solution of bio-based modified films (BMF), methacrylic acid (MA) was used as a reactive diluent, 2,2-dimethoxy-2-

phenylacetophenone (DMPA) as a photoinitiator, and tetra (ethylene glycol) diacrylate (TEGDA) as a cross-linker. They were added to the ML-Ma before curing with UV radiation. By examining the intensity of the C=C peak appearing at 1635 cm^{-1} in the FTIR spectrum, the approximate curing percentage was calculated. A methyl ethyl ketone (MEK) rub test was also conducted to check the crosslinking of the UV-cured sample.

The BMF films were prepared with varying amounts of bio-based content ranging from 0 wt. % to 55 wt. % (BMF-0 to BMF-55) to reduce the amount of commercial cross-linker (TEGDA). The UV-cured films were investigated to study their mechanical and thermal properties. Good results were obtained using 30 wt. % of ML-Ma (BMF-30). An increase in tensile strength, hardness, and flexural characteristics was observed. The variation in the amounts of TEGDA and ML-Ma showed the bio-content needed to optimize the mechanical properties of the film. As a result of this study, it was found that commercial products TEGDA cross-linker can be partially replaced by modified bio-based content of ML-Ma with increasing the overall mechanical properties of the films.

TABLE OF CONTENTS

CHAPTER PAGE

I. INTRODUCTION………………………………………………………………………… 1

- 1.1. Polymeric films…………………………………………………………………… 1
  - 1.1.1. Types of polymeric films………………………………………………… 3
    - 1.1.1.1. Thermoplastics …………………………………………………… 3
    - 1.1.1.2. Thermosets ………………………………………………………… 4
    - 1.1.1.3. Elastomers ………………………………………………………… 4
- 1.2. Compositions in film formulation…………………………………………… 4
  - 1.2.1. Types of resins…………………………………………………………… 5
    - 1.2.1.1. Polyacrylic resin…………………………………………………… 6
  - 1.2.2. Crosslinkers……………………………………………………………… 8
  - 1.2.3. Photoinitiator…………………………………………………………… 9
  - 1.2.4. Reactive diluent………………………………………………………… 10
- 1.3. Curing method…………………………………………………………………… 11
  - 1.3.1. Thermal curing…………………………………………………………… 11
  - 1.3.2. UV curing………………………………………………………………… 11
- 1.4. Bio-based films…………………………………………………………………… 12
  - 1.4.1. Synthesis of bio-based UV-curable films and coatings…… 12
- 1.5. Research objective……………………………………………………………… 13

II. EXPERIMENTAL DETAILS……………………………………………………………… 15

- 2.1. Materials ………………………………………………………………………… 15
- 2.2. Synthesis…………………………………………………………………………… 20
  - 2.2.1. Synthesis of limonene diol ……………………………………… 20
  - 2.2.2. Synthesis of methacrylated limonene diol ………………… 21
  - 2.2.3. Curing process ………………………………………………………… 21
- 2.3. Characterizations……………………………………………………………… 22
  - 2.3.1. Titration………………………………………………………………… 23
    - 2.3.1.1. Iodine value……………………………………………………… 23
    - 2.3.1.2. Hydroxyl value…………………………………………………… 23
  - 2.3.2. Fourier transforms infrared spectroscopy………………… 23
    - 2.3.2.1. Cure percentage………………………………………………… 24
  - 2.3.3. Thermo gravimetric analysis………………………………………… 24
  - 2.3.4. Viscosity measurement……………………………………………… 25
  - 2.3.5. Gel permeation chromatography………………………………… 26
  - 2.3.6. MEK rub test……………………………………………………………… 27
  - 2.3.7. Mechanical properties……………………………………………… 27
    - 2.3.7.1. Tensile strength ……………………………………………… 27

2.3.7.2. Flexural strength ………………………………………………… 28
2.3.7.3. Hardness…………………………………………………………………. 29
2.3.8. Chemical resistivity …………………………………………………….. 30

III. RESULTS AND DISCUSSION………………………………………………………. 31

3.1. Synthesis……………………………………………………………………………. 31
3.1.1. Synthesis of limonene diol ……………………………………….. 31
3.1.1.1. Gel permeation chromatography………………………….. 32
3.1.1.2. Iodine value…………………………………………………………. 32
3.1.1.3. Hydroxyl value…………………………………………………….. 33
3.1.1.4. Fourier transforms infrared spectroscopy …………….. 33
3.1.2. Synthesis of methacrylated limonene diol …………………. 34
3.1.2.1. Hydroxyl value………………………………………………………. 35
3.1.2.2. Fourier transforms infrared spectroscopy……………….. 35
3.1.3. Curing formulation……………………………………………………. 36
3.1.3.1. Components in curing formulation………………………….. 36
3.1.3.2. Possible cross-linked structure of BMF…………………… 37
3.2. Characterizations……………………………………………………………………. 38
3.2.1. Digital photos of bio-based modified film……………………… 38
3.2.2. Fourier transforms infrared spectroscopy………………………. 38
3.2.3. MEK rub test………………………………………………………………… 40
3.2.4. Thermo gravimetric analysis………………………………………… 41
3.2.5. Mechanical properties……………………………………………….. 43
3.2.5.1. Tensile strength ………………………………………………….. 44
3.2.5.2. Flexural strength ………………………………………………… 44
3.2.5.3. Hardness…………………………………………………………………. 45
3.2.6. Chemical resistivity…………………………………………………….. 48

IV. CONCLUSION…………………………………………………………………………. 50

FUTURE WORK……………………………………………………………………………. 51

REFERENCES……………………………………………………………………………….. 52

LIST OF TABLES

TABLE PAGE

Table 1.1 Types of photochemical reactions…………………………………………………. 10

Table 2.1 Formulas for bio-based films……………………………………………………… 22

Table 3.1 Cure percentages of BMF………………………………………………………… 40

Table 3.2 TGA data for each cured BMF……………………………………………………. 42

Table 3.3 Test results of tensile, flexural, and hardness testing ……………………… 43

Table 3.4 Loss of weight (%) in acid, water, and base solution……………………… 49

LIST OF FIGURES

FIGURE PAGE

Figure 1.1 Chemical structure of acryl group………………………………………….. 6

Figure 1.2 Structure of poly MA and poly MMA……………………………………… 7

Figure 1.3 Vulcanized natural rubber……………………………………………………… 8

Figure 1.4 Radical generation of DMPA…………………………………………………… 10

Figure 2.1 Chemical structure of limonene………………………………………………. 15

Figure 2.2 Chemical structure of 2- mercaptoethanol……………………………. 16

Figure 2.3 Chemical structure of 1-methacrylic anhydride……………………… 16

Figure 2.4 Chemical structure of 2-hydroxy-2-methylpropiophenone.......... 17

Figure 2.5 Chemical structure of dimethoxy-2-phenylacetophenone ……….. 17

Figure 2.6 Chemical structure of 1-methylimidazole………………………………. 18

Figure 2.7 Chemical structure of tetra (ethylene glycol) diacrylate…………… 18

Figure 2.8 Chemical structure of methacrylic acid………………………………….. 18

Figure 2.9 Chemical structure of tetrahydrofuran…………………………………. 19

Figure 2.10 UV instruments……………………………………………………………………. 20

Figure 2.11 Instrument of Fourier transforms infrared spectroscopy…………. 24

Figure 2.12 TGA instrument…………………………………………………………………… 25

Figure 2.13 TA Instrument rheometer ……………………………………………………… 26

Figure 2.14 GPC instrument……………………………………………………………………. 27

Figure 2.15 Tensile instrument……………………………………………………………….. 28

Figure 2.16 Flexural instrument……………………………………………………………… 29

Figure 2.17 Type D Durometer for hardness test …………………………………….. 30

Figure 3.1 Synthesis of limonene diol …………………………………………………… 31

Figure 3.2 GPC curves of limonene diol and limonene………………………… 32

Figure 3.3 FTIR for limonene and limonene diol ………………………………….. 34

Figure 3.4 Synthesis of methacrylated limonene diol ……………………… 35

Figure 3.5 FTIR for LD and ML-Ma ………………………………………………………… 36

Figure 3.6 Possible cross-linked structure of BMF………………………………….. 37

Figure 3.7 BMF cured film…………………………………………………………………….. 38

Figure 3.8 The intensity of C=C before and after UV curing for each BMF…. 39

Figure 3.9 MEK rub test on BMF film…………………………………………………… 40

Figure 3.10 Curves of (a)TGA (b) DTGA of BMFs ………………………………………. 43

Figure 3.11 Tensile strength for BMFs……………………………………………………… 44

Figure 3.12 Flexural strength for BMFs…………………………………………………… 45

Figure 3.13 Hardness for BMFs………………………………………………………………… 46

Figure 3.14 Comparisons of tensile, flexural, and hardness for BMFs…………. 47

Figure 3.15 Image of BMF films after 24 hours in acid, water, and base solutions………………………………………………………………………… 48

CHAPTER I

INTRODUCTION

Polymeric films have been important to society as they can improve product life by protecting it through daily wear and tear. The primary function of a cured film is to protect coated materials by reducing corrosion or decomposition. With the chemical modification of the raw material, different functions like adhesion, chemical and heat-resistance, and anti-corrosion can be obtained. Diverse classes of film formulations are commercially available and developed by researchers that are used in unusual weather, underwater, and space applications to protect material as needed. Petroleum-based raw materials are used in film formation but due to their limited sources, researchers are looking for alternative green materials and approaches to synthesize polymeric films.

1.1 Polymeric Films

Polymeric materials that are thicker than 200 µm are known as a sheet [1]. Typical uses of polymeric films span over the household, industrial, and high-tech applications like packaging, bags, automotive, aerospace, construction, and landscaping. Based on the properties of polymeric resin from which the polymeric films have been prepared can be transparent, semi-transparent, opaque, colored, smooth, or rough, and used in different applications depending upon their physio-chemical, thermal, and mechanical properties. In general, plastic films are used to separate the area or volume, act as a barrier, hold the materials, and offer printable surfaces. Other sectors where polymeric films are applied include the manufacture of sensors, biomedical devices, and tuning of the surface’s wettability, adhesion, friction, and wear [2].

Polymeric films can be thermoplastic, thermoset, or elastomeric which are prepared using different methods such as blown film extrusion, calendaring, casting through polymer solution or dispersion, and radiation curing. The most common polymers used in the preparation of films are polyethylene (low, high, and ultra-high density), polypropylene, polyurethane, polyester, nylon, poly (vinyl chloride), poly (vinyl alcohol), cellulose acetate, and biodegradable synthetic polymers like poly(l-lactide), polyglycolide, poly(ε-caprolactone), and their co-polymers. Many of the natural and synthetic bio-polymers are also used as an additive in film formulation to improve their rate of biodegradation and physio-chemical properties [3][4]. In general, the biomass-derived monomers may be oxygen-rich (lactic acid and succinic acid), hydrocarbon (bio-olefins), non-hydrocarbon (carbon dioxide), and hydrocarbon-rich (vegetable oils, fatty acids, and terpenes) can be used in the synthesis of bio-film [5]. In this research, limonene is used as bio-based material which is extracted from the abundantly available citrus fruit. The presence of an electron-donating group on the double bonds through hyperconjugation in the limonene opens the pathways for easily accessible chemical reactions to synthesize the polymers and other useful chemical compounds [6]. Free radical copolymerization of limonene is also possible with other monomers or polymers which are reported in many research [7].

The worldwide biopolymer films market is predicted to grow at a compound annual growth rate (CAGR) of 8.4% from 2022 to 2028, with a value of USD 4 billion in 2021 [8].

1.1.1. Types of polymeric films

Films are made up of long-chain molecules composed of many repeating units known as monomers. They are mainly divided into three groups: Thermoplastics, Thermosets, and Elastomers.

1.1.1.1. Thermoplastics

Thermoplastic films are based on materials that soften to a liquid when heated and solidify when cooled. The presence of monomers or polymers and additives in the film causes the above properties. The manufacturing of these plastic resins is useful for commercial and industrial purposes such as in automobile parts, making sports equipment, and toys. A wide range of thermoplastic films can be synthesized including polycarbonate, polyurethanes, and acrylic resins to obtain various properties like flexibility, impact resistivity, and transparency [9]. These films can be found in consumer items such as packaging and storage materials and as an insulator in electronic equipment.

1.1.1.2. Thermosets

Thermoset films are prepared by curing different types of resin, such as epoxy, polyesters, polyurethane, vinyl esters, and acrylic-based resins. Curing is initiated by the use of heat or other suitable radiation to generate crosslinked polymers. Hardeners, fillers, curing agents, and isocyanates are some of the materials used with these resins to increase their mechanical and thermal properties [10]. Thermoset polymers are commonly used in construction equipment, kitchen appliances, and motor components.

1.1.1.3. Elastomers

Elastomer-based films exhibit elasticity and revert to their original form after distortion. These types of films can be composed of epoxy, polyurethane, acrylic, and silica-based resins [11]. Due to their flexibility, insolubility, and elasticity, elastomers are used in different types of industries like construction, food processing, and automotive.

1.2. Compositions in film formulation

Resins, cross-linkers, photoinitiators, reactive diluents, and many more components are used in the film formulation [12]. Resins are used to create polymer chains that can then be joined together to form a film. This process is called polymerization. The resulting film has specific properties, such as strength and flexibility, that depend on the type of monomers used and the conditions of the polymerization reaction. In the synthesis of films, crosslinkers are added to the polymer solution to help the polymer chains join together to form a continuous film. This process is called cross-linking. Some examples of crosslinkers that are used in the synthesis of films include epoxy resins and multifunctional acrylates. Most of the multifunctional acrylates are used to create films that are clear and strong and they are often used in the production of transparent packaging materials.

When the film formulation is exposed to light, the photoinitiator is used to absorb the light energy and transforms it into chemical energy, and initiate the photopolymerization reaction. they are commonly used in the production of films, as well as in other applications such as 3D printing and inkjet printing. A reactive diluent is a chemical compound that is added to the curing formulation during the synthesis of films. These compounds can be added to this formulation to reduce its viscosity.

Each component plays a role in altering the specific characteristics in terms of the chemical, rheological, thermal, mechanical, and physical properties. Another additive including pigments can be used in film formation. Pigments are used to colorize the film and improve its reflectiveness.

1.2.1. Types of resins

A UV-curable resin can be a natural or synthetic material that used in curing formulations. Many different types of resins, including epoxy, polyurethane, polycarbonate, polyacrylic, phenolic, alkyd, polyamide, and silicone resins, are employed. Different types of resin are used in film formulation and each resin has its own chemical properties. Resin takes an important role in film formulation where functional groups crosslink with another or the same monomer. With an increase in the degree of crosslinking, the strength of the film also increases. Resins are frequently utilized in engineering as adhesives and coatings when adhesion is required to the surface. For usage of film for coating purposes, acrylic resins are mostly used for weather resistance [13], alkyd resins for moisture resistance [14], epoxy for resistance to heavy-duty corrosion [15], phenolic for high-temperature applications [16], polyesters as a protective layer and good chemical resistance [17], and silicate-based resins as a binding agent in a film to improve coating surface adhesion [18].

1.2.1.1. Polyacrylic resin

Acrylic resin is a kind of thermosetting material commonly made from the monomers of acrylic acid, methacrylic acid, or acrylate-based compounds. An acryl group is shown in **Figure 1.1**.

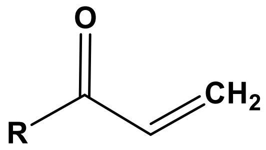

Figure 1.1. Chemical structure of acryl group.

The esters of acrylic and methacrylic acid are known as acrylic monomers. Methyl, ethyl, isobutyl, 2-ethylhexyl, and n-butyl are a few examples of typical esters. Functional groups like amide groups (acrylamide) [19], amino groups (dimethylamino ethyl methacrylate) [20], and hydroxyl groups (hydroxyl ethyl methacrylate) [21] can be found in the esters. Different types of functionalities give different types of improvement in mechanical and thermal properties. **Figure 1.2.** shows two polymer structures that have only functionality differences of the methane group. **Figure 1.2.** also shows different mechanical properties [22].

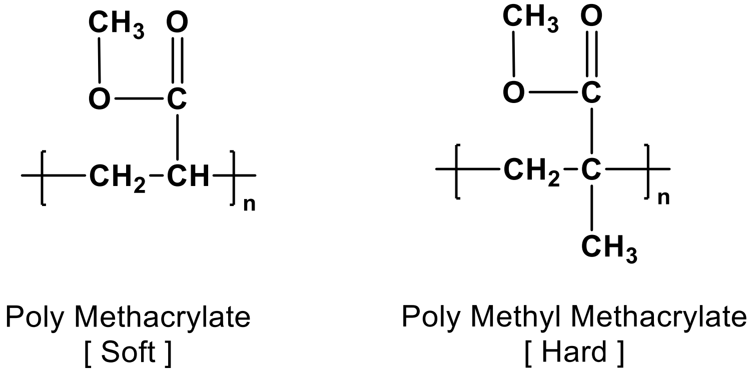

Figure 1.2. Structure of poly MA and poly MMA.

Acrylic resins can be polymerized by bulk, solution, suspension, and emulsion polymerization. Acrylic resin-based polymers are commercially available and have multiple coating properties like stain and water resistance, adhesion, toughness, scratch resistance, and resistance to solvent [23]. Polyacrylates can be used for coating, adhesives, and films among many other applications due to their transparency, shiny appearance, and strong cohesiveness [24].

In an experiment by researcher Guo et.al, a micelle solution of POSS-based fluorinated acrylate polymer was mixed with ethyl-a-cyanoacrylate to form the film. This film shows super hydrophobic properties with good durability [25].

1.2.2. Crosslinkers

As the name describes, a crosslinker is used for crosslinking the polymer chains in curing formulation which increases physical properties like strength and rigidity of the polymer material. Homofunctional cross-linking reagents create a framework in which two or more pendant groups make a bond by interacting with each other [26]. On the other hand, heterobifunctional cross-links are produced by using two or more different functional groups to make a crosslinked structure in a polymer [27].

The vulcanization of natural rubber with sulfur, two polymer chains cross-linked in a polymeric matrix, as seen in **Figure 1.3**, is a typical example of cross-linking. To cross-link a polymer effectively, it is reported to utilize either dynamic (reversible) covalent bonds or irreversible covalent bonds. In the presence of a dynamic crosslinker, the polymer matrix has the flexibility to modify its structural configuration due to the reversibility of dynamic covalent bonds that can be repaired or broken [28]. In irreversible covalent bonding, linkages remain the same under different chemical conditions.

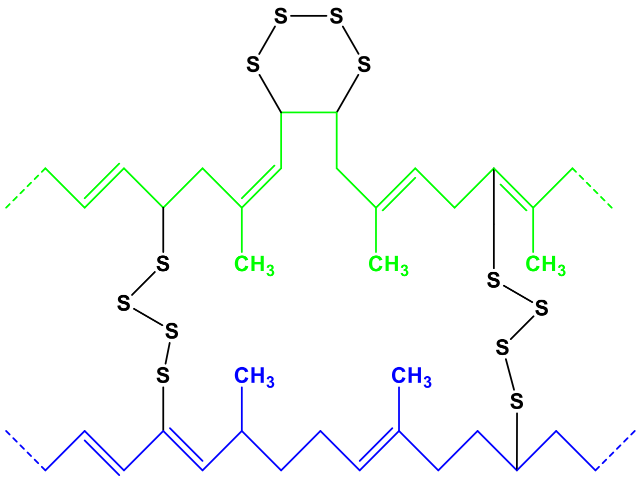

Figure 1.7. Vulcanized natural rubber.

Many mechanisms, including click chemistry, coupling of amides, photopolymerization, alkene cyclization, and others have been used to create this type of cross-linking [29]. *Songqi et. al.* utilize a bio-based tetra functional gallic acid-based crosslinker in the photopolymerization synthesis to see any changes in the properties of the polymer. The UV-curing method was used to crosslink the acrylated epoxidized soybean oil (AESO) with this bio-based crosslinker. Crosslinked AESO networks showed higher crosslink density, gel content, and tensile strength. Thus, a bio-based crosslinker can be used in place of a petroleum-based crosslinker [30][31].

1.2.3. Photoinitiator

Photoinitiators are molecules that absorb photons and activate molecules to an excited state upon radiation of light, which aid in starting subsequent processes of photopolymerization. In the photolysis process, extra energy from the excited state breaks the bond of the molecule into two pieces and promotes further reaction. However, in an excited state, molecules can isomerize with nearby molecules and release energy through relaxation or emission. Multiple reactions can be observed including an excited state (*) [32], which is shown in **Table 1.1.**

Table 1.1. Types of photochemical reactions.

Name of the reaction	Function	Possible route
Photolysis	Bond breakage and generate free radicals	A–B–C* → A–B• + C•
Photosensitization	Every form of energy is transfer	A–B–C* + D → A–B–C+D*
Photosensitization	Electron transfer	A–B–C* + D → A–B–C^+ + D^-

For example, 2, 2-dimethoxy-2-phenylacetophenone (DMPA) is used as an initiator to begin the photochemical reaction. As shown in **Figure 1.4**, the initiator will create radicals when exposed to light and these radicals will then start the process of radical polymerization. This initiator is mostly employed in the preparation of acrylate-based polymers [33].

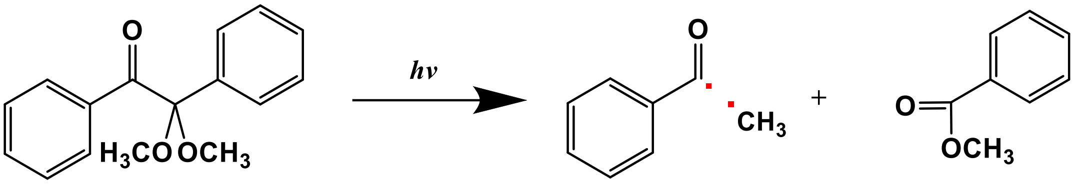

Figure 1.4. Radical generation of DMPA.

1.2.4. Reactive diluent

To facilitate film formulations, reactive diluents (thinners) are typically used to make resins less viscous. Reactive diluents assist the formulation by enabling the inclusion of additional fillers and enhancing substrate-wetting behavior. Reactive diluents are divided into monofunctional and polyfunctional categories. When compared to di-functional and multi-functional reactive diluents, monofunctional reactive diluents often demonstrate better ductility and a reduction in the modulus of the cured film [34]. A lot of reactive diluents are based on acrylates and styrene. Commercially, the reactive diluent of Epodil® 750 is often used to reduce the viscosity of epoxy-based resins and to take part in the resulting cured crosslinked polymer [35].

1.3. Curing method

Mainly two methods are used to cure the films: Thermal and UV-curing.

1.3.1. Thermal curing

The most widely used method of curing polymer composites is thermal curing. Many different thermal heating systems are used for thermal curing, including molten, microwave, laser, flame, oven, induction, ultrasonic, and more. Radiation heating (microwave and laser) works by converting electromagnetic radiation into heat as a result of molecules' resonance vibrations at a certain radiation wavelength. The principle of combustion heating (molten, flame, and oven) is the flow of gases or liquids between surfaces to transfer heat. In the electromagnetic induction method (induction thermal curing), heat is transferred through an induction coil. This produces an electromagnetic field inside the coil and cures the solution on the material. Autoclaves are the most common thermal curing method and are widely used in the manufacturing of thermoset composites. This curing method has two drawbacks including lengthy curing processes with higher consumption of energy, and, uncured or degradation in curing by failure to maintain a constant temperature.

1.3.2. UV curing

This curing is performed by ultraviolet radiation. This is cost-effective, user-friendly, and requires low energy. With radiation curing, photo-initiators activate the chemical reaction under the influence of UV light. Radical photo-polymerization takes place to cure the formulation after it is applied on the substrate. During this process, radiation crosslinks the monomer or polymer, causing it to change phases from a liquid to a solid. This method happens very quickly and helps to reduce production time. No solvents are typically needed to complete this process which makes it eco-friendly and attracts researchers as well as manufacturers. UV curing has more advantages compared to thermal curing because it does not require an oven, takes less time to cure, and is easy to use as a portable device. UV curing is often applied to photo lithography, coating, and printing.

1.4. Bio-based films

Bio-based films are made up to varying degrees of monomers extracted from natural sources like plants, vegetables, or fruits. Examples are monomers such as limonene, lignin, eugenol, and various types of carbohydrates. They have potential uses in formulations for films. Low-cost plant essential oils have many reactive groups including phenolic, hydroxyl, allyl, and aromatic rings. In order to achieve the desirable properties, the chemical modification takes place via forming and breaking these bonds, and a solution can be formulated and prepared for end-use applications. The bio-based resins can be epoxy, acrylate, polyester-based, and many more.

1.4.1. Synthesis of bio-based UV-curable films and coatings

For example, bio-based eugenol acrylate film was successfully synthesized by *Zheng et al.* [36] for film coating and 3D printing. Eugenol is extracted from clove which is also known as clove oil [37]. In their research, new environmentally friendly, solvent-free bio-based acrylates were synthesized. Siloxane groups were introduced to eugenol via a hydrosilylation reaction. In hydrosilylation, Si-H addition happens by breaking the double bond of eugenol. Furthermore, an acrylation reaction takes place to make a UV-curable solution which is used in coating and printing with the addition of a photoinitiator. Cured bio-based film gives a good result with increased hydrophobicity and higher thermal stability by using surface analysis and thermogravimetric analysis, respectively. Film also showed good crosslinking by performing gel contents.

1.5. Research objective

The objective of this research was to increase the bio-based content in film formulations to make bio-based films by using UV light. Limonene is extracted from the peels of citrus fruits [38]. In the thiol-ene reaction, limonene (L) reacts under UV radiation to produce a high yield of limonene diol. Subsequently, a methacrylation reaction was used to formulate methacrylated limonene diol for film formation. With the increased amount of bio-based content, a liquid BMF formulation was cured under UV radiation. The bio-based modified film (BMF) was tested for thermal, and mechanical properties. They were also characterized by studying crosslinking and chemical resistivity.

CHAPTER II

EXPERIMENTAL DETAILS

2.1. Materials

In this research, the listed below materials used in synthesis and their chemical structure are shown in **Figures 2.1 to 2.9.**

Limonene

The chemical structure of limonene ($C_{10}H_{16}$) is shown in **Figure 2.1**. Limonene is a cyclic monoterpene class of aliphatic hydrocarbon that is in liquid form. D-limonene, in particular, is extracted from citrus peels to make edible oils [38]. This compound has a molecular weight of 136.24 g/mol. Limonene was used as a bio-material for coating.

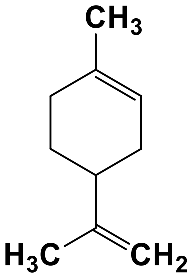

Figure 2.1. Chemical structure of limonene.

2- Mercaptoethanol

The chemical structure of 2- mercaptoethanol (C_2H_6OS) is shown in **Figure 2.2**. This compound has a molecular weight of 78.13 g/mol. It was used as a reactant in thiol-ene reaction.

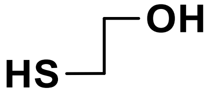

Figure 2.2. Chemical structure of 2- mercaptoethanol.

1-Methacrylic anhydride

The chemical structure of 1-methacrylic anhydride ($C_8H_{10}O_3$) is shown in **Figure 2.3**. This compound has a molecular weight of 154.165 g/mol. It was used as a reactant in a methacrylation reaction.

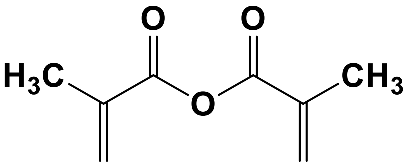

Figure 2.3. Chemical structure of 1-methacrylic anhydride.

2-Hydroxy-2-Methylpropiophenone

The chemical structure of 2-hydroxy-2-methylpropiophenone ($C_{10}H_{12}O_2$) is shown in **Figure 2.4**. This compound has a molecular weight of 164.20 g/mol. It was used as a photoinitiator in thiol-ene reaction.

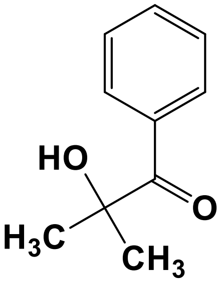

Figure 2.4. Chemical structure of 2-hydroxy-2-methylpropiophenone.

Dimethoxy-2-phenylacetophenone

The chemical structure of dimethoxy-2-phenylacetophenone ($C_{16}H_{16}O_3$) is shown in **Figure 2.5.** This compound has a molecular weight of 256.301 g/mol. It was used as a photoinitiator in curing formulation.

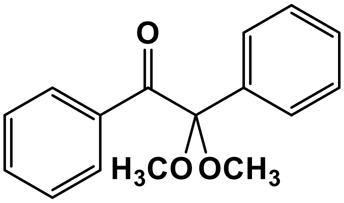

Figure 2.5. Chemical structure of dimethoxy-2-phenylacetophenone.

1-Methylimidazole

The chemical structure of 1-methylimidazole ($C_4H_6N_2$) is shown in **Figure 2.6**. This compound has a molecular weight of 82.10 g/mol. It was used as a catalyst in a methacrylation reaction.

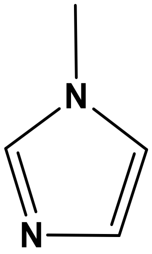

Figure 2.6. Chemical structure of 1-methylimidazole.

Tetra (ethylene glycol) diacrylate

The chemical structure of tetra (ethylene glycol) diacrylate ($C_{14}H_{22}O_7$) is shown in **Figure 2.7**. This compound has a molecular weight of 302.32 g/mol. It was used as a crosslinking monomer in curing formulation.

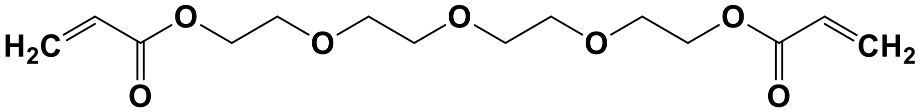

Figure 2.7. Chemical structure of tetra (ethylene glycol) diacrylate.

Methacrylic acid

The chemical structure of methacrylic acid ($C_4H_6O_2$) is shown in **Figure 2.8**. This compound has a molecular weight of 86.09 g/mol. It was used as a reactive diluent in curing formulation.

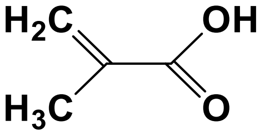

Figure 2.8. Chemical structure of methacrylic acid.

Tetrahydrofuran

The chemical structure of tetrahydrofuran (C_4H_8O) is shown in **Figure 2.9**. This compound has a molecular weight of 72.107 g/mol. It was used as a solvent in a methacrylation reaction.

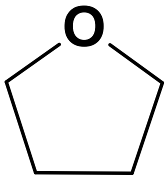

Figure 2.9. Chemical structure of tetrahydrofuran.

UV source

Two types of UV sources were used in this research: UV-1 and UV-2 in **Figure 2.10**. UV-1 is equipped with 20 watts of mercury lamp from Analytik Jena (Upland, CA, USA). UV-2 is equipped with 400 watts of UVA-enhanced metal halide lamp from Uvitron international (West Springfield, MA, USA).

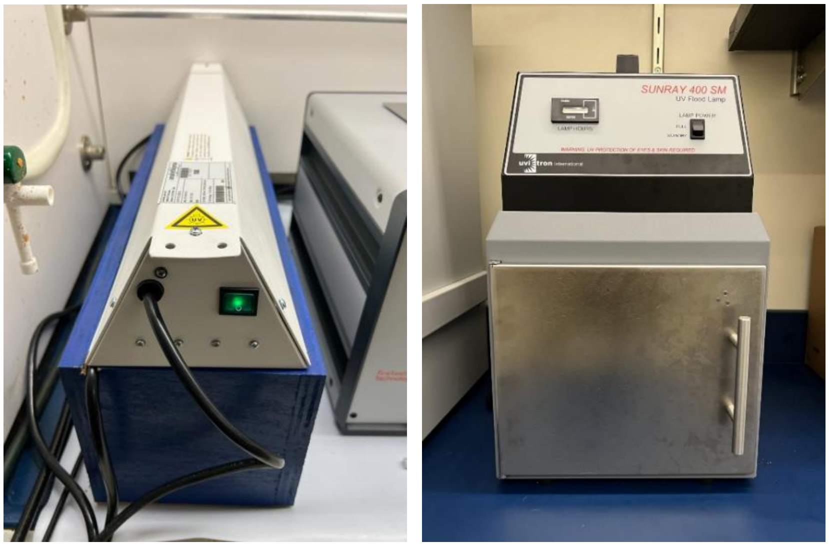

Figure 2.10. UV instruments.

2.2 Synthesis

2.2.1. Synthesis of limonene diol

By thiol-ene reaction, limonene and 2-mercaptoethanol were reacted to produce limonene diol in the presence of a photoinitiator and UV-1 radiation. In this reaction, 2-mercaptoethanol (2 mol) was added to limonene (1 mol) in a 500 ml flask. A photoinitiator of 2-hydroxy-2-methylpropiophenone (0.012 mol) was added to above solution to begin the reaction and placed under UV light (365 nm) for 5 hours at ambient temperature. The yield of this reaction is limonene diol (LD) and it is a yellowish liquid. FTIR analysis, titration methods and gel permeation chromatography technique were used to characterize the synthesized LD.

2.2.2. Synthesis of methacrylated limonene diol

limonene diol (0.5 mol) was dissolved in (400 ml) in THF. The solution was thoroughly stirred for 15 minutes in three-neck round bottom flask equipped with a condenser, thermometer, and a mechanical stirrer, under a nitrogen atmosphere. Next, 1-methylimidazole (0.11 mol) was added into 1-methacrylic anhydride (1 mol) and then added dropwise into the above solution for 30 minutes. The temperature was then increased to 50 °C and the reaction was stirred for 3 hours. Finally, THF was removed using rotary evaporation. The yield of this reaction is methacrylated limonene diol (MaLD). FTIR analysis and titration methods were used to characterize the synthesized MaLD.

2.2.3. Curing process

To prepare for curing, a photo-initiator of DMPA, a cross-linking agent of TEGDA, and a reactive diluent of MA were added to ML-Ma. ML-Ma is a mixture of MaLD and a byproduct of methacrylic acid from methacrylation reaction. The amount of DMPA and the excess amount of MA is constant in formulation. Excess amounts of MA reduce viscosity from 1.7 to 0.11 Pa.s. The weight percentage of the crosslinker is decreased in samples in order to increase the bio content, to evaluate the effectiveness of a bio-based compound (**Table 2.1**). The mixture of curing formulation refers to a BMF whereas BMF-0 means 0 wt.% of ML-Ma.

In this curing formulation, a reactive diluent was used to reduce the viscosity of this solution. During the curing, added photoinitiator DMPA absorbs the photon energy from UV light. Radical polymerization takes place in this formulation. By this process bio-content MaLD gets cross-linked with TEGDA. This polymerization generates a cross-linked structure in the polymer matrix and cured the film.

Table 2.1. Formulas for bio-based films.

Sample	**ML-Ma**	**TEGDA**	**DMPA**	**MA**	**Total (wt.%)**
BMF-0	0	57	5	38	100
BMF-10	10	47	5	38	100
BMF-20	20	37	5	38	100
BMF-30	30	27	5	38	100
BMF-35	35	22	5	38	100
BMF-40	40	17	5	38	100
BMF-45	45	12	5	38	100
BMF-55	55	2	5	38	100

2.3 Characterizations

Various wet chemistry and spectroscopic methods were used to characterize the starting and synthesized materials. The American Society for Testing and Materials (ASTM) and the International Organization for Standardization (ISO) methods were used for the characterization of synthesized materials. **Figures 2.11 to 2.20** display the instruments used for characterizations.

2.3.1. Titration

2.3.1.1. Iodine value (I.V.)

Iodine reacts effectively with a double bond or triple bond present in an unsaturated compound. By identifying the iodine number, changes in the concentration of double bonds or triple bonds can be observed. The Hanus titration method (IUPAC 2.205) was used to determine the iodine number for limonene and synthesized product.

2.3.1.2. Hydroxyl value

The hydroxyl number (OH-value) is used to determine the amount of the hydroxyl groups, which is contained by compound or diol. To obtain the OH-value for the limonene diol and methacrylated limonene diol, the phthalic anhydride pyridine (PAP) method was used in accordance with IUPAC 2.241.

2.3.2. Fourier transforms infrared spectroscopy

By using the fast and effective technique of Fourier transforms infrared spectroscopy (FTIR), a variety of functional groups can be detected. This analysis uses infrared light to scan the samples of organic, inorganic, and polymeric compounds to identify various bond absorptions intrinsic to certain functional groups. Changes in the final product can be detected by studying the intensity of the absorbance peaks. By calculating the differences in intensity of C=C around 1635 cm^{-1} [39], the cure percentage can be determined. A PerkinElmer Spectrum Two Spectrophotometer was used to collect FT-IR spectra at room temperature with a range of 4000-400 cm^{-1} (**Figure 2.11**).

Figure 2.11. Fourier transforms infrared spectrometer.

2.3.2.1. Cure percentage

To calculate the cure percentage, the FTIR peak, and the equations below are used. By knowing the percent transmittance, absorbance can be determined by equation (1) and then used in equation (2) to find the cure percentage (C%).

$$A = 2 - \log(\%T) \quad \text{.............} \ (1)$$

$$C\,\% = \frac{(A_0 - A_t)}{A_0} \times 100\% \quad \text{...........} \ (2)$$

Where, A= Absorbance, $\%T$= percent transmittance, C %= Cure percentage, A_0= Absorbance before curing, and A_t= Absorbance after curing.

2.3.3. Thermogravimetric analysis

In thermogravimetric analysis, the thermal stability is observed for BMF films. TA instrument (TGA Q500 Discovery, Trios, USA) was used for thermogravimetric analysis

(**Figure 2.12.**). Under a nitrogen atmosphere, samples were heated from 25 to 700 °C at a ramping temperature of 10 °C per minute.

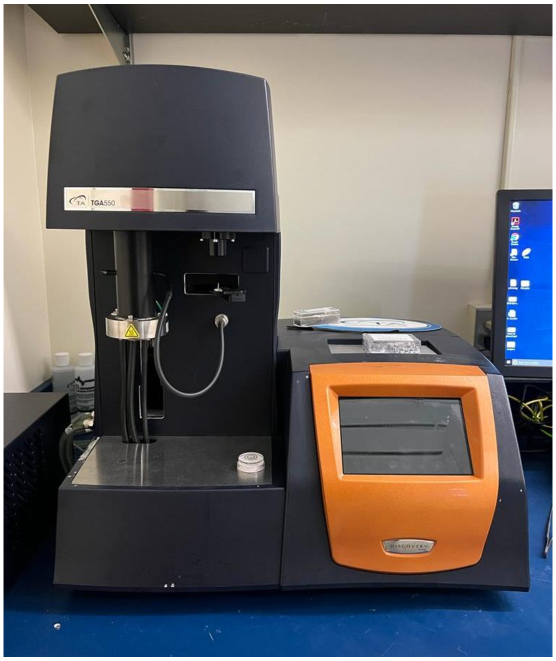

Figure 2.12. TGA instrument.

2.3.4. Viscosity measurement

Viscosity is a key factor in any fluid dynamic measurements. Due to ease of application, lower viscosity liquid is preferred for end-use applications. Using a TA Instruments rheometer (**Figure 2.13.**), the viscosity of the samples was investigated at room temperature. A cone plate with a 2° angle and a 25 mm cone diameter was attached to the dynamic rheometer at 25 °C. Viscosity was monitored with a linearly increasing shear stress from 1 to 2000 Pa.

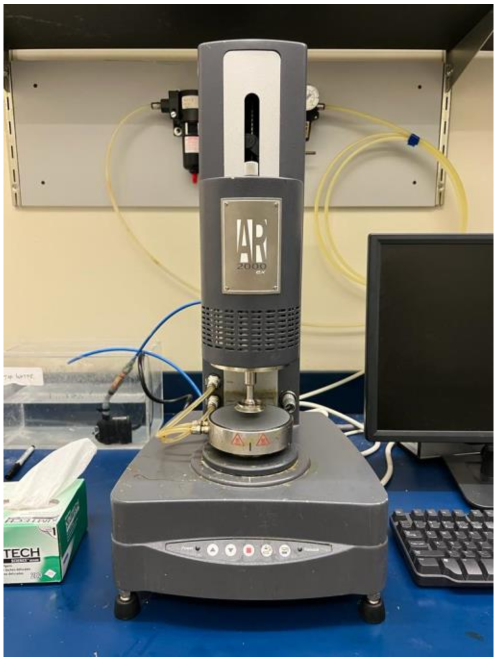

Figure 2.13. TA Instrument rheometer

2.3.5. Gel permeation chromatography

Gel permeation chromatography is used to analyze compounds a mixture by separating them based on molecular size which is also known as size exclusion chromatography. The water GPC instrument was used (**Figure 2.14**) with 4 phenogel 5µ columns (300 × 7.8 mm) containing various pore sizes of 50, 102, 103, and 104. THF was used as the eluent solvent, and the flow rate was 1 ml/min at 30 °C.

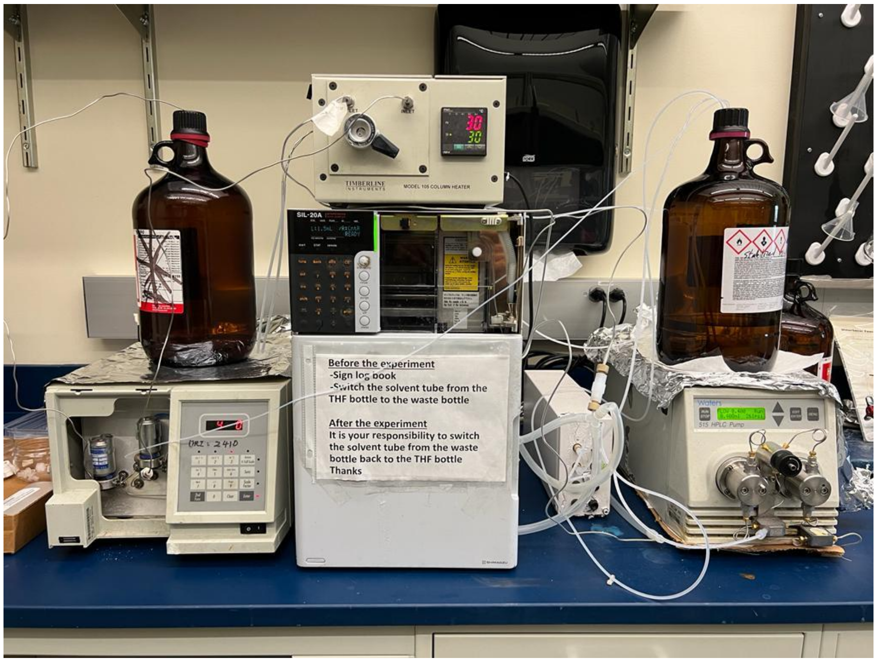

Figure 2.14. GPC instrument

2.3.6. MEK rub test

The MEK rub test is a solvent resistance test. After UV curing, samples were left at room temperature for 24 hours prior to performing the test. It was used to verify crosslinking by visualizing the film's surface. After performing the rub test, a scrape or dissolved surface of the cured film was observed. A cotton swab was dipped in the MEK solvent and immediately rubbed 10 times back and forth on the cured film.

2.3.7. Mechanical properties

2.3.7.1. Tensile strength

Tensile strength is defined as the maximum stress that a material can handle before breaking when pulled or stretched. An instrument grasps a piece of material at both ends and slowly pulls it vertically until it breaks. The breaking point is considered the sample's maximum tensile strength. An Instron Model 3367 (Instron, USA) with a crosshead speed of 50 mm/min was used to measure the tensile strength (**Figure 2.15**). The provided results for the tensile strength under maximum load are the average value obtained from tests made on three different samples.

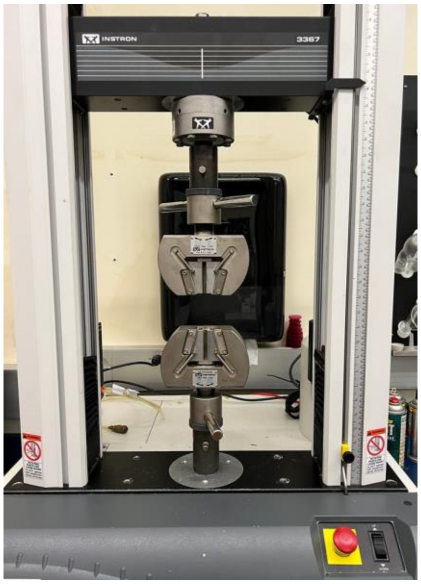

Figure 2.15. Tensile instrument

2.3.7.2. Flexural strength

A flexural test is performed to analyze mechanical properties where the 3-point banding technique (**Figure 2.16.**) is used to determine the modulus of elasticity while bending for the cured film. The provided results for the banding modulus are the average values obtained from tests made on three different specimens. To calculate the modulus of bending, the equation below is used according to ASTM D-790.

$$\text{Flexural strength} \quad \boldsymbol{E_B} = \frac{\boldsymbol{L^3}\mathbf{m}}{\mathbf{4b}\boldsymbol{d^3}}$$

Where, E_B= modulus of elasticity in bending (Flexural strength), L= length of the support span, m= slope of the tangent, b= width of the sample, and d= thickness of the sample.

Figure 2.16. Flexural instrument

2.3.7.3. Hardness

Hardness is one of the more important factors in film properties which is used in the study of impact-resistance. Hardness testing was performed by applying the appropriate load to penetrate the film. The Type D Durometer (PTC instruments) was used to determine hardness according to ASTM D2240 (**Figure 2.17**). This instrument has a sharp point at the bottom and is used to puncture the cured film by applying force. Hardness can be observed on the dial.

Figure 2.17. Type D Durometer for hardness test

2.3.8. Chemical resistivity

To examine the chemical resistance on the cured film, acid, water, and base medium are generally used. The cured film is dipped in the solution of those three mediums for 24 hours to see if any decomposition or deformation takes place. The weight of the sample was recorded before and after testing to notice any weight changes. The performance of a cured film was examined using three different aqueous solutions which are categorized by pH; 1N HCl (pH=1, acid), water (pH=7, neutral), and 1N NaOH (pH=14, base). All samples were submerged in those mediums for 24 hrs.

CHAPTER III

RESULTS AND DISCUSSION

3.1. Synthesis

3.1.1. Synthesis of limonene diol

By thiol-ene reaction, limonene diol was synthesized where limonene reacted with 2-mercaptoethanol (2-ME) in presence of 2-hydroxy-2-methylpropiophenone photoinitiator under UV radiation. This photoinitiator-catalyzed reaction promotes S-H bond cleavage resulting in the formation of sulfur (S•) radical. By radical addition of sulfur (-S) to the double bond of limonene, a carbon-sulfur (C-S) bond formed (**Figure 3.1**). This reaction is also known as alkene hydrothiolation where thiol (R-SH) and alkene (R′C=CR′) form thioether (R-S-R′) [40].

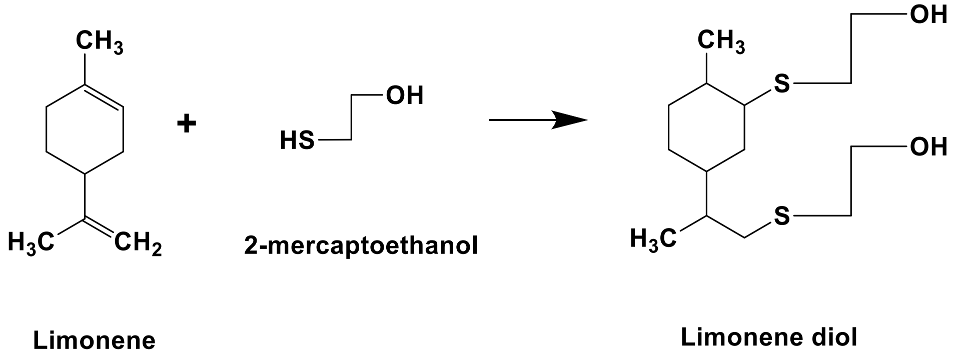

Figure 3.1. Synthesis of limonene diol.

3.1.1.1. Gel permeation chromatography

According to the GPC curves of limonene and limonene diol, the majority of the limonene was transformed into diol. This can be seen in **Figure 3.2.** The limonene diol peak at 26.6 minutes has a higher molecular weight than the limonene peak at 29.6 minutes due to the decrease in retention time.

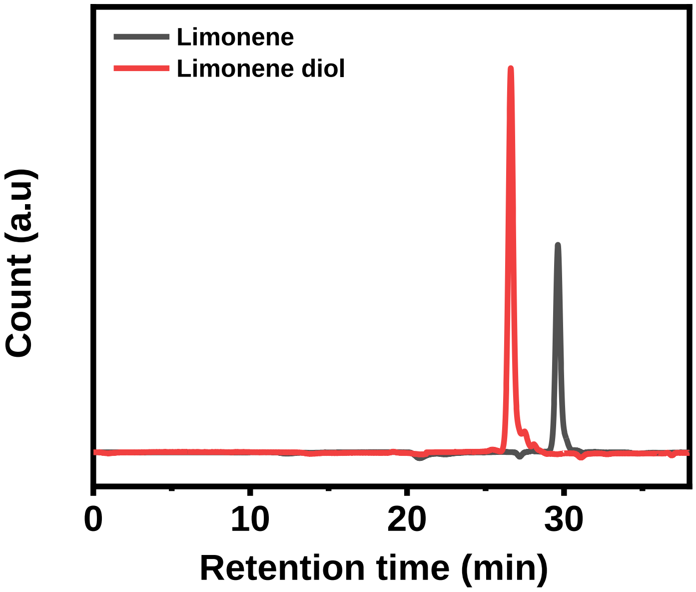

Figure 3.2. GPC curves of limonene diol and limonene.

3.1.1.2. Iodine value

An iodine value of 355.09 g I_2/100g was recorded for the limonene which changed to 3.1 g I_2/100g for the diol. This confirmed the consumption of the double bond in order to introduce the -OH functionality contained by 2-mercaptoethanol.

3.1.1.3. Hydroxyl value

The hydroxyl value of LD is also determined by titration. The observed OH value at 275.16 mg KOH/g confirms that the -OH groups are present in LD, which were not present in the raw material (limonene).

3.1.1.4. Fourier transforms infrared spectroscopy

Figure 3.3 shows the FTIR spectra of the bio-based raw material limonene and the resulting product of LD. In the spectrum of limonene, the C=C peak was observed at 1635 cm^{-1} which indicates the presence of a double bond whereas, for 2-ME, the S-H bond is represented by the vibration band at 2560 cm^{-1} [41]. The resulting product of LD was analyzed by absorbance peaks whereas the peak around ~3340 cm^{-1} show the -OH stretch in diol due to the forming of -OH groups in the thiol-ene reaction [42]. For LD, the C=C and S-H peaks disappeared and the OH group appeared, which is consistent with the synthesis of LD.

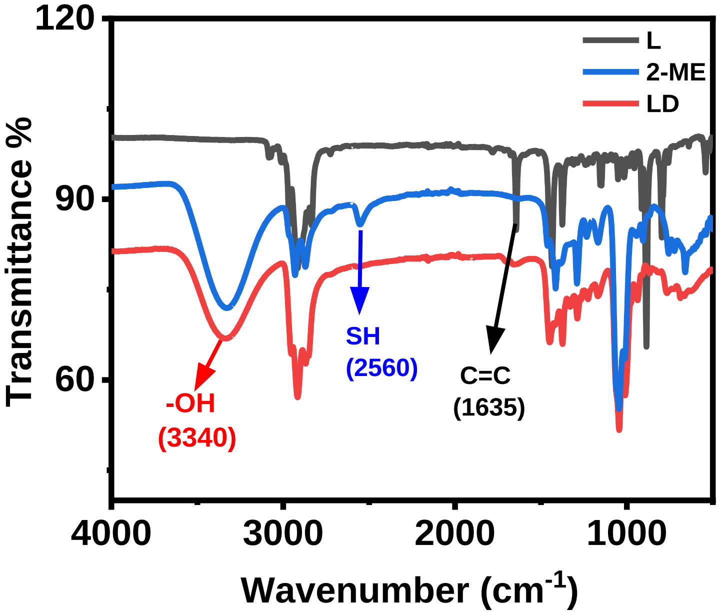

Figure 3.3. FTIR for limonene and limonene diol.

3.1.2. Synthesis of methacrylated limonene diol

A methacrylation reaction was used to synthesize MaLD via the esterification of limonene diol with methacrylic anhydride. The OH group is transformed into an ester along with cleavage of the anhydride (**Figure 3.4.**). The cleavage of the anhydride is seen in many reactions [43]. The advantage of the 1-methylimidazole catalyst over acid catalysts is that it is both more active and selective. One of the LD's terminal alcohol groups attacks the methacrylic anhydride's carbonyl and generates a methacrylic acid byproduct. In this synthesis, methacrylic anhydride was used instead of methacryloyl chloride, which is more frequently utilized. Methacrylic acid is the byproduct created when LD reacts with methacrylic anhydride as opposed to the triethylamine/HCl salt that is produced when LD reacts with methacrylic chloride [44]. Methacrylic anhydride was preferred in these processes because the byproduct of methacrylic acid can be used as a reactive diluent to reduce viscosity instead of removing the salt byproduct.

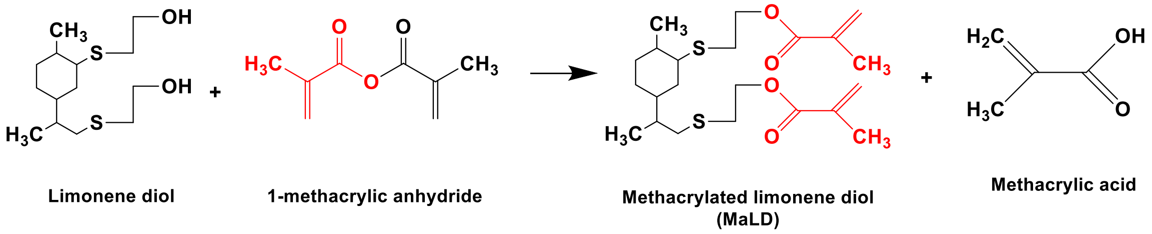

Figure 3.4. Synthesis of methacrylated limonene diol.

3.1.2.1. Hydroxyl value

During the reaction, the hydroxyl group was transferred into an acrylic group. The OH value was decreased from 275.16 mg KOH/g (from LD) to 4.7 mg KOH/g for MaLD, which confirms that the hydroxyl group was reduced in the reaction.

3.1.2.2. Fourier transforms infrared spectroscopy

According to FTIR analysis, (**Figure 3.5**), the absorbance peak at 1635 cm^{-1} shows the acrylic double bond on limonene diol whereas the OH group disappears at 3340 cm^{-1} [42]. In this reaction, a byproduct of methacrylic acid also shows one broad peak in the FTIR spectrum for the carboxyl functional groups (-COOH) [45]. The presence of acrylic double bonds confirmed the synthesis of MaLD.

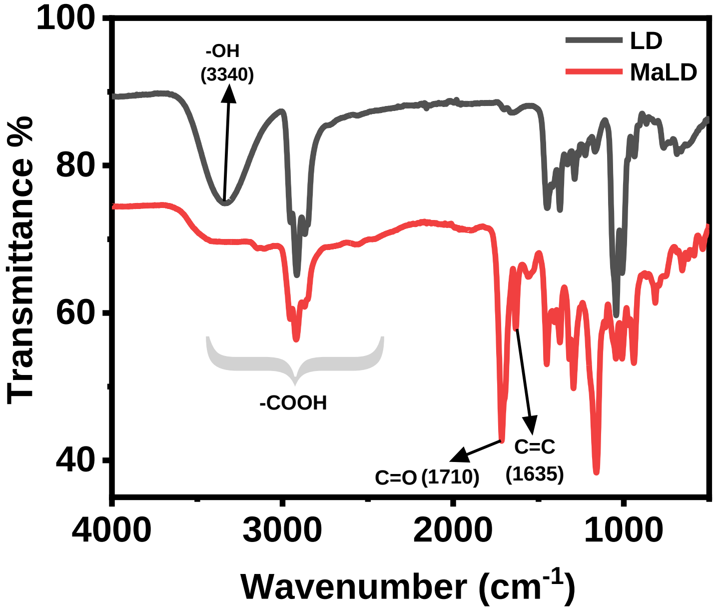

Figure 3.5. FTIR for LD and MaLD.

3.1.3. Curing formulation

3.1.3.1. Components in curing formulation

The composition for each curing formulation is shown in **Table 2.1**. In this formulation, bio-based modified MaLD was added up to 55 wt.% to see its effects on the properties of the cured film. A commercial cross-linker TEGDA was used in decreasing amounts with an increasing amount of MaLD. For characterization, 0 wt.% of MaLD (BMF-0) solution was cured under UV radiation and the cured film was tested and evaluated with an increased amount of MaLD (BMF-10 to BMF-55) film. For ease of application, a reactive diluent of methacrylic acid was used to reduce the viscosity of the formulation from 1.7 to 0.11 Pa.s. The amount of the photoinitiator DMPA used was 5 wt.% to initiate a curing reaction under UV radiation. The radicalization of DMPA is shown in **Figure 1.4**. MA and DMPA were both used in a constant amount for each formulation.

FT-IR analysis, TGA, and MEK rub, tensile, flexural, hardness, and also chemical resistivity (effect) tests were conducted on 0.8 mm thick cured film. The mechanical test required thicker films for testing. In this research, they were cast in a Petri dish due to ease of removal and used for testing. The 0.8 mm thickness of the films was maintained by adding 10g of product into a Petri dish and curing for 8 seconds using the UV-2.

3.1.3.2. Possible cross-linked structure of BMF

After UV-curing, acrylic double in MaLD takes part in cross-linking and cures the BMF film. A possible cross-linked structure of BMF is shown in **Figure 3.6**.

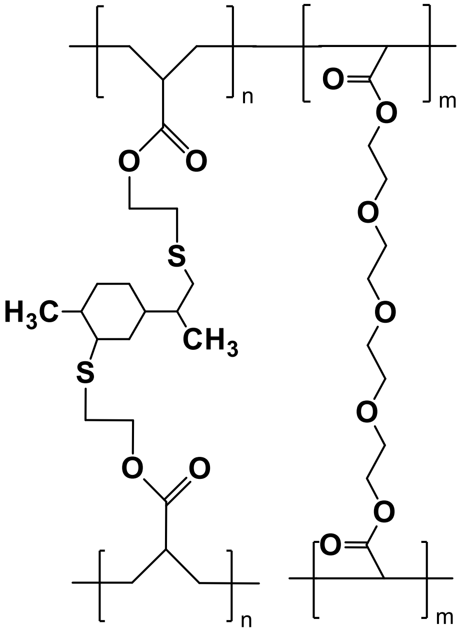

Figure 3.6. Possible cross-linked structure of BMF.

3.2. Characterizations

3.2.1. Digital photos of bio-based modified film

Cured BMF film was used in this research to characterize the properties like thermal, mechanicals, and chemical resistivity (**Figure 3.7**).

Figure 3.7. BMF cured film.

3.2.2. Fourier transforms infrared spectroscopy

FTIR spectra were taken to analyze the curing process and determine the cure percentage for UV-cured solid film (BMF). Curing involves the creation of linear C-C bonds by opening the C=C bonds. In **Figure 3.8**, after curing, the absorbance peak of acrylic C=C shows a reduction at 1635 cm^{-2} [39]. The difference between the intensity of C=C before and after curing presents the cure percentage. Results are shown in **Table 3.1**. The cure percentage can be determined by comparing the before and after cured spectra of the BMF. The cure rates for all BMF films were found to be remarkably high above 90%.

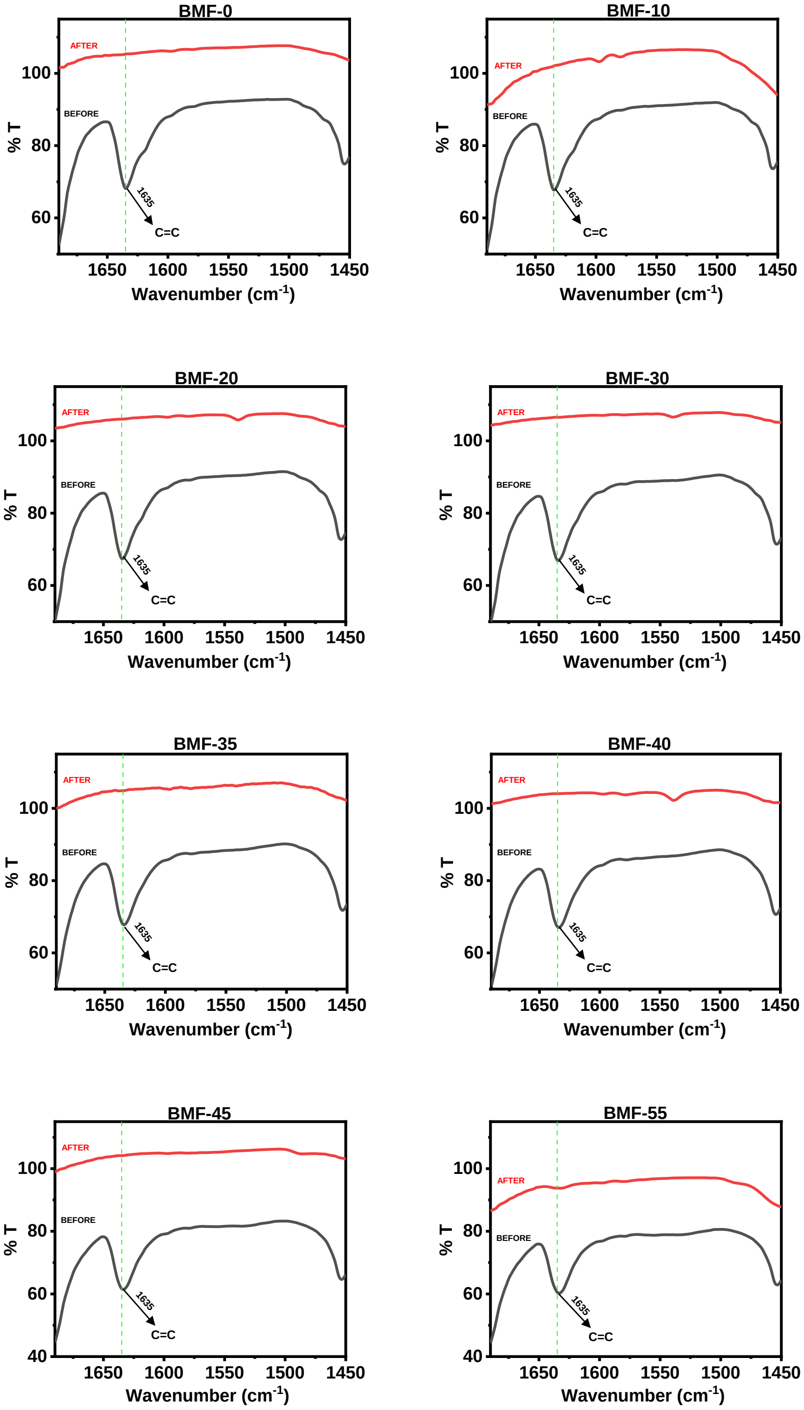

Figure 3.8. The intensity of C=C before and after UV curing for each BMF.

Table 3.1. Cure percentages of BMF.

SAMPLE	CURE PERCENTAGE [%]
BMF-0	92.44
BMF-10	90.77
BMF-20	92.30
BMF-30	92.30
BMF-35	92.00
BMF-40	92.16
BMF-45	92.30
BMF-55	90.90

3.2.3. MEK rub test

After performing the MEK (solvent) rub test, if a scrape or dissolved surface is observed it means the film has lower crosslinking and still needs further UV radiation. Curing time can be determined by this test. All cured films from BMF-0 to BMF-55 were tested and no scrape or dissolved surface was observed (**Figure 3.9.**), indicating that all films were cross-linked properly and the cure time was sufficient.

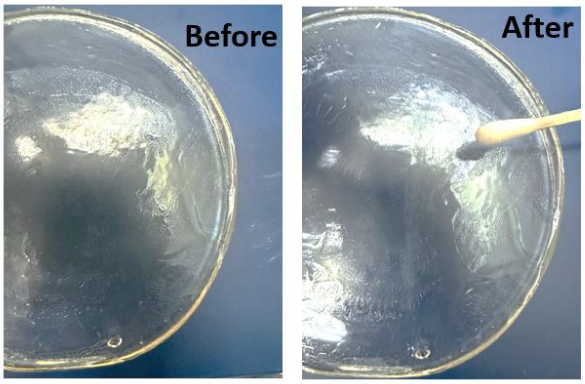

Figure 3.9. MEK rub test on BMF film.

3.2.4. Thermogravimetric analysis

The influence of the modified bio-based content on the thermal stability of the films as examined.

Based on the TGA graph (**Figure 3.7**), two stages of decomposition were observed. 2 % weight loss of the material can be observed around 183-192 ℃ . The initial (**Table 3.2.**) or first decomposition stage (T_{id}) is around 160-250 ℃. This can be attributed to the breakdown of the glycol content in the TEGDA cross-linker. This stage of decomposition shows the degradation of glycol [46].

The second stage of decomposition (T_{sd}) occurs around 415-453 ℃. This is indicative of the breakdown of the acrylic backbone, typically recorded at temperature below 460 ℃ via a depolymerization process [47].

The same thermal stability of the material can be observed in the Derivative of TGA (DTGA curve). The decomposition of the material occurred in first and second stage, which is ascribed to glycol and acrylate degradation, respectively.

Table 3.2. TGA data for each cured BMF.

Sample	Initial decomposition temperature (℃)	Second decomposition temperature (℃)
BMF-0	187.34	425.6
BMF-10	192.4	419.47
BMF-20	187.4	416.94
BMF-30	183.55	415.03
BMF-35	191.94	416.86
BMF-40	191.55	421.15
BMF-45	188.24	453.95
BMF-55	184.95	425.71

All samples of BMF exhibit similar thermal stability in terms of 2% weight loss. Therefore, bio-content exhibit similar effect in crosslinking process. This indicates comparable behavior of bio-content as a cross-linker aside to the commercial cross-linker, TEGDA. Thus, it is shown that bio-based MaLD may be used as a cross-linker in the formulation of the film.

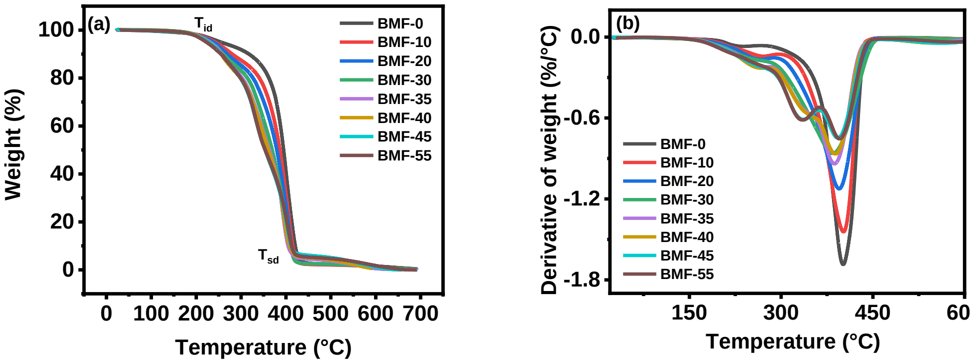

Figure 3.10. Curves of (a)TGA (b) DTGA of BMFs.

3.2.5. Mechanical properties

Cured films of BMF-0 to BMF-55 were analyzed by mechanical testing. The data from tensile, flexural, and hardness testing follow a similar pattern with increasing bio-based MaLD. The summary of the result is shown in **Table 3.3**.

Table 3.3. Test results of tensile, flexural, and hardness testing.

Sample	Tensile strength (MPa)	Flexural strength (GPa)	Hardness (D)
BMF-0	64.37	16.80	84
BMF-10	68.69	25.10	85
BMF-20	75.17	27.46	86
BMF-30	79.43	38.10	88
BMF-35	47.32	32.61	85
BMF-40	21.00	25.70	84
BMF-45	1.86	21.14	75
BMF-55	0.64	16.95	34

3.2.5.1. Tensile strength

During the tensile test, the displacement is transformed into a strain value, and the load is transformed into a stress value. This data is used to determine the tensile strength. For each BMF film, three (3) specimens were used in testing and an average value was reported. The respective tensile strengths of BMF-0 to BMF-55 are shown below in **Figure 3.11.**

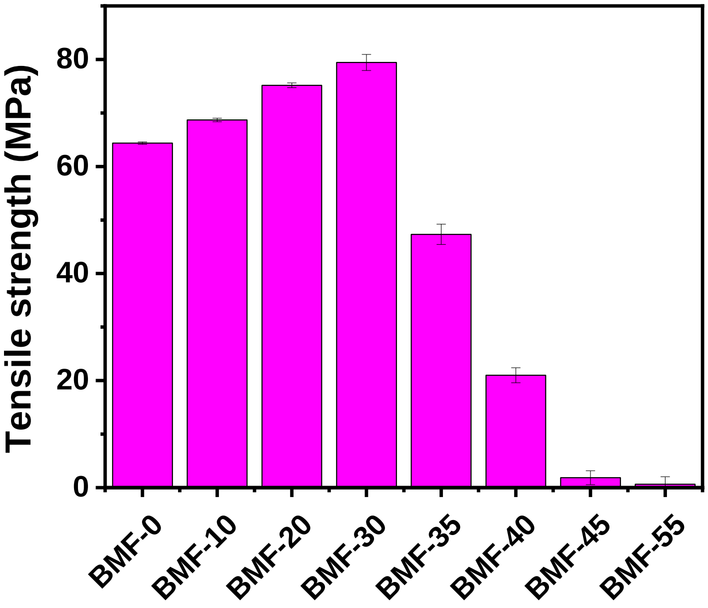

Figure 3.11. Tensile strength for BMFs.

3.2.5.2. Flexural strength

To determine the flexural strength via bending, the ratio of stress to strain in flexural deformation is used. The material with 30 wt.% of bio-based content (BMF-30) shows the highest flexural strength but when the amount of MaLD exceeds 30 wt.%, the resulting films became brittle. The flexural strength increased up to 30 wt. % and then started decreasing in the range from 30 to 55 wt. %. This is shown below in **Figure 3.12**.

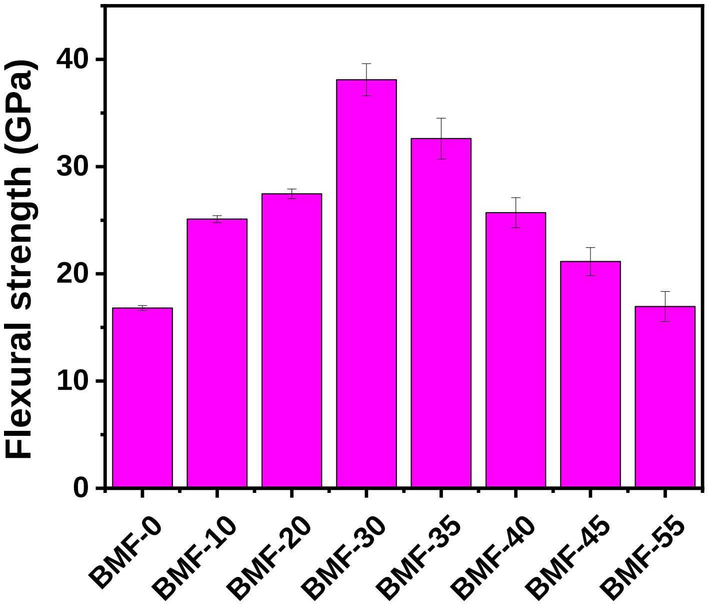

Figure 3.12. Flexural strength for BMFs.

3.2.5.3. Hardness

A hardness test measures a material's penetration by another material. Similar to the flexural testing the hardness of the material increased from BMF-0 to BMF-30 but then decreased from BMF-30 to BMF-55. This is shown in **Figure 3.13**.

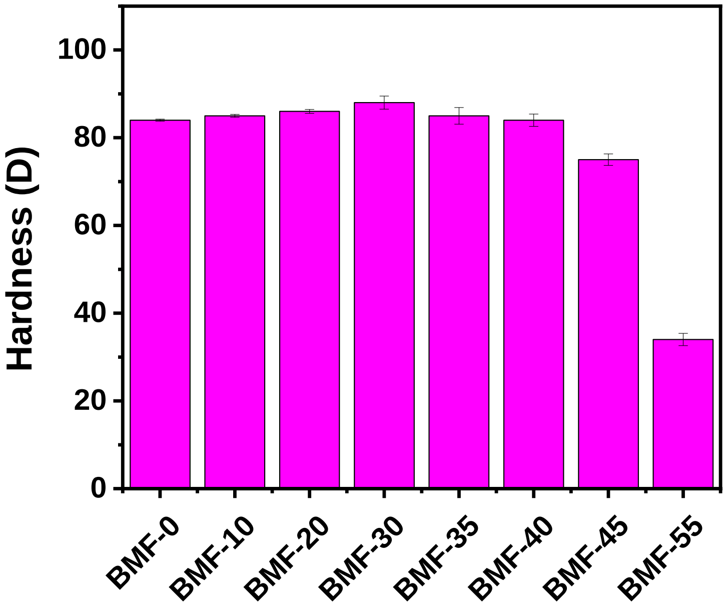

Figure 3.13. Hardness for BMFs.

Increased bio-based content from 0 wt.% to 30 wt.% shows improvement in tensile strength but further decreases for 35 wt.% to 55 wt.%. The same trends follow in the flexural strength as well as in the hardness, which is shown in **Figure 3.14**. Mechanical strength was reduced because the cured film became more brittle after the addition of 35% bio-content. The bulky group is a reason that brittleness increases with increasing bio-based content. MaLD contains a bulky group which restricts the rotational motion, reducing the flexibility of the chain and causing brittleness [48][49].

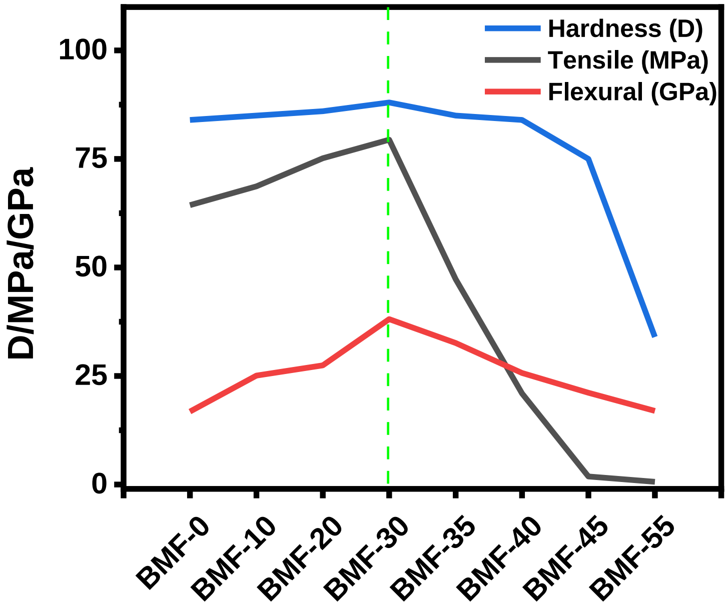

Figure 3.14. Comparisons of tensile, flexural, and hardness for BMFs.

Another factor might be affecting brittleness is the stiffening group like carbonyl [50]. MaLD and TEGDA also carry a carbonyl group which stiffens the polymer by reducing the flexibility of the polymer chain. The combined effect of the bulky group and carbonyl group in film increase the brittleness. This effect is also shown in the results of tensile strength, flexural strength, and hardness (**Table 3.3**).

3.2.6. Chemical resistivity

Chemical resistivity is an important factor in film performance. The effect of a cured film for all BMF samples was examined under three different acidities; 1N HCl, water, and 1N NaOH. All samples were socked under those mediums for 24 hr. The before and after weights of the samples were collected in terms of loss of weight (%) and shown in **Table 3.4**. During the test, the deformation of cured film was observed in a base solution and a picture of the sample under these three mediums is shown in **Figure 3.15**.

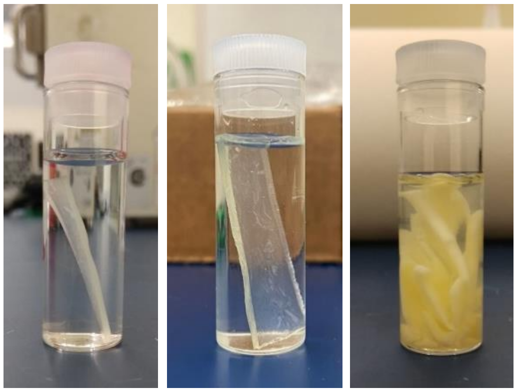

Figure 3.15. Image of BMF films after 24 hours in acid, water, and base solutions (left to right).

Table 3.4. Loss of weight (%) in acid, water, and base solution.

Sample	ACID	WATER	BASE
BMF-0	1.21%	2.79%	25.39%
BMF-10	1.19%	2.31%	27.62%
BMF-20	1.19%	2.25%	31.47%
BMF-30	1.17%	1.85%	37.98%
BMF-35	1.09%	1.41%	43.55%
BMF-40	1.02%	1.19%	49.91%
BMF-45	0.76%	0.83%	56.38%
BMF-55	0.64%	0.58%	63.95%

As per the result, bio-based modified films show excellent acid-resistance properties. The reason is that before curing, the curing solution shows 4 pH which is acidic in nature because bio-content contains acid content. As more acid content increases in the film, it tries to neutralize in the base solution and react with NaOH. In the base solution, acid content from the film chemically reacts with NaOH and makes sodium acetate. Generally, a reaction between carboxylic acid and sodium hydroxide produces sodium acetate and water. In this case, might be this reaction takes place and deformation observed in **Figure 3.15**. This leads to higher weight loss in the base medium. Under acid, the lowest weight loss was observed whereas, in water, slightly more loss of weight was shown in **Table 3.4.**

CHAPTER IV

CONCLUSION

Limonene was successfully modified using thiol-ene and methacrylation reactions. The synthesized methacrylated limonene diol was characterized and evaluated for its performance in films. Under UV radiation, the BMF films were successfully cured, which were composed of varying amounts of bio-based content ranging from 0 wt. % to 55 wt. %. By investigating the intensity of C=C peak in the FTIR spectrum, more than 90% of curing was observed in all BMF films whereas cross-linking is also confirmed by the MEK rub test. The film consisting of 30 wt.% bio-based content displayed higher mechanical performance. With the increase in bio content from 35 wt.% to 55 wt.%, bulky groups generate the brittleness in the films, respectively. The brittle structure of the films further reduces their mechanical properties as stress is applied to them. The thermal stability was not compromised with the increase in bio content as observed in the TGA results. This suggests that MaLD could be a potential alternative for the commercial crosslinker of TEGDA.

FUTURE WORK

The primary goal of this research was to replace commercial petroleum products by increasing the quantity of bio-based substances in film formulations. Another aspect of this research is that it might be used for 3D printing to print resin layer by layer. This study could be expanded in the future to make the changes and improvements listed below.

1) Try different modified bio-based compounds to see their performance in the film (like in this research acrylic double bonds were introduced to the bio-based compound).

2) To make a more flexible and less brittle film, less bulky and stiffing groups contained compounds could be used like soybean oil (which is used in the synthesis of flexible polyurethane film).

REFERENCES

1. Drobny JG (2020) 1 - Introduction. In: Drobny JGBT-A of FF (ed) Plastics Design Library. William Andrew Publishing, pp 3–38
2. Carroll GT, Sojka ME, Lei X, Turro NJ, Koberstein JT (2006) Photoactive Additives for Cross-Linking Polymer Films: Inhibition of Dewetting in Thin Polymer Films. Langmuir 22:7748–7754
3. Tang X, Alavi S (2011) Recent advances in starch, polyvinyl alcohol based polymer blends, nanocomposites and their biodegradability. Carbohydr Polym 85:7–16
4. Patil S, Bharimalla AK, Mahapatra A, Dhakane-Lad J, Arputharaj A, Kumar M, Raja ASM, Kambli N (2021) Effect of polymer blending on mechanical and barrier properties of starch-polyvinyl alcohol based biodegradable composite films. Food Biosci 44:101352
5. Yao K, Tang C (2013) Controlled Polymerization of Next-Generation Renewable Monomers and Beyond. Macromolecules 46:1689–1712
6. Wilbon PA, Chu F, Tang C (2013) Progress in Renewable Polymers from Natural Terpenes, Terpenoids, and Rosin. Macromol Rapid Commun 34:8–37
7. Ranaweera CK, Ionescu M, Bilic N, Wan X, Kahol PK, Gupta RK (2017) Biobased Polyols Using Thiol-Ene Chemistry for Rigid Polyurethane Foams with Enhanced Flame-Retardant Properties. J. Renew. Mater. 5
8. Kiran P, Sayan M (2022) Biopolymer Films Market Size, Share and Industry Analysis Report. Global Market Insights Inc GMI205:350

9. Wazarkar K, Kathalewar M, Sabnis A (2016) Reactive Modification of Thermoplastic and Thermoset Polymers using Flame Retardants: An Overview. Polym Plast Technol Eng 55:71–91

10. Luo L, Meng Y, Qiu T, Li X (2013) An epoxy-ended hyperbranched polymer as a new modifier for toughening and reinforcing in epoxy resin. J Appl Polym Sci 130:1064–1073

11. Mammeri F, Bourhis E Le, Rozes L, Sanchez C (2005) Mechanical properties of hybrid organic–inorganic materials. J Mater Chem 15:3787–3811

12. Porter SC (2021) Chapter 27 - Coating of pharmaceutical dosage forms. In: Adejare ABT-R (Twenty-third E (ed) Remington-Elsevier. Elsevier Wordmark-ScienceDirect, Academic Press, pp 551–564

13. Jiao C, Sun L, Shao Q, Song J, Hu Q, Naik N, Guo Z (2021) Advances in Waterborne Acrylic Resins: Synthesis Principle, Modification Strategies, and Their Applications. ACS Omega 6:2443–2449

14. Aulin C, Ström G (2013) Multilayered Alkyd Resin/Nanocellulose Coatings for Use in Renewable Packaging Solutions with a High Level of Moisture Resistance. Ind Eng Chem Res 52:2582–2589

15. Zhang Z, Zhao N, Qi F, Zhang B, Liao B, Ouyang X (2020) Reinforced Superhydrophobic Anti-Corrosion Epoxy Resin Coating by Fluorine–Silicon–Carbide Composites. MDPI, Coatings 10(12):1244

16. Huang J, Fu S, Gan LBT-LC and A (2019) Chapter 6 - Lignin-Modified

Thermosetting Materials. Elsevier, pp 163–180

17. Motlatle AM, Ray SS, Ojijo V, Scriba MR (2022) Polyester-Based Coatings for Corrosion Protection. MDPI, Polym. 14:3413

18. Hoshyargar F, Ali Sherafati S, Hashemi MM (2009) A new study on binder performance and formulation modification of anti-corrosive primer based on ethyl silicate resin. Prog Org Coatings 65:410–413

19. Beaudoin G, Lasri A, Zhao C, Liberelle B, De Crescenzo G, Zhu X-X (2021) Making Hydrophilic Polymers Thermoresponsive: The Upper Critical Solution Temperature of Copolymers of Acrylamide and Acrylic Acid. Macromolecules 54:7963–7969

20. Shalati MD, Scott RM (1975) Thermal Polymerization of Dimethylaminoethyl Methacrylate. Macromolecules 8:127–130

21. Brantley EL, Jennings GK (2004) Fluorinated Polymer Films from Acylation of ATRP Surface-Initiated Poly(hydroxyethyl methacrylate). Macromolecules 37:1476–1483

22. George B. Kauffman ANG, Bierwagen GP, Stevens MP, Preston J, Rodriguez F (2022) Acrylic polymers. Major Ind. Polym. 5 :2-56

23. Sickler D (2002) Water-based Alchemy. In: Dundean Stud. 6:56-87

24. Huang K, Liu Y, Wu D (2014) Synthesis and characterization of polyacrylate modified by polysiloxane latexes and films. Prog Org Coatings 77:1774–1779

25. Guo D, Chen J, Wen L, Wang P, Xu S, Cheng J, Wen X, Wang S, Huang C, Pi P

(2018) A superhydrophobic polyacrylate film with good durability fabricated via spray coating. J Mater Sci 53:15390–15400

26. Aiertza MK, Odriozola I, Cabañero G, Grande H-J, Loinaz I (2012) Single-chain polymer nanoparticles. Cell Mol Life Sci 69:337–346

27. Hiki S, Kataoka K (2007) A Facile Synthesis of Azido-Terminated Heterobifunctional Poly(ethylene glycol)s for “Click” Conjugation. Bioconjug Chem 18:2191–2196

28. Wojtecki RJ, Meador MA, Rowan SJ (2011) Using the dynamic bond to access macroscopically responsive structurally dynamic polymers. Nat Mater 10:14–27

29. Mavila S, Eivgi O, Berkovich I, Lemcoff NG (2016) Intramolecular Cross-Linking Methodologies for the Synthesis of Polymer Nanoparticles. Chem Rev 116:878–961

30. Ma S, Jiang Y, Liu X, Fan L, Zhu J (2014) Bio-based tetrafunctional crosslink agent from gallic acid and its enhanced soybean oil-based UV-cured coatings with high performance. RSC Adv 4:23036–23042

31. Gillani SS, Munawar MA, Khan KM, Chaudhary JA (2020) Synthesis, characterization and applications of poly-aliphatic amine dendrimers and dendrons. J Iran Chem Soc 17:2717–2736

32. Vione D, Maurino V, Minero C, Pelizzetti E, Harrison MAJ, Olariu R-I, Arsene C (2006) Photochemical reactions in the tropospheric aqueous phase and on particulate matter. Chem Soc Rev 35:441–453

33. Liao K-C, Hogen-Esch T, Richmond FJ, Marcu L, Clifton W, Loeb GE (2008) Percutaneous fiber-optic sensor for chronic glucose monitoring in vivo. Biosens Bioelectron 23:1458–1465
34. Phalak G, Patil D, Vignesh V, Mhaske S (2018) Development of tri-functional biobased reactive diluent from ricinoleic acid for UV curable coating application. Ind Crops Prod 119:9–21
35. Evonik Industries AG (2022) MONO- AND DIFUNCTIONAL REACTIVE DILUENTS. Evonik Oper. 3:21
36. Zheng J, Cai Y, Zhang X, Wan J, Fan H (2022) Eugenol-Based Siloxane Acrylates for Ultraviolet-Curable Coatings and 3D Printing. ACS Appl Polym Mater 4:929–938
37. Khalil AA, Rahman U ur, Khan MR, Sahar A, Mehmood T, Khan M (2017) Essential oil eugenol: sources, extraction techniques and nutraceutical perspectives. RSC Adv 7:32669–32681
38. Lopresto CG, Petrillo F, Casazza AA, Aliakbarian B, Perego P, Calabrò V (2014) A non-conventional method to extract D-limonene from waste lemon peels and comparison with traditional Soxhlet extraction. Sep Purif Technol 137:13–20
39. Fu J, Liu W, Hao Z, Wu X, Yin J, Panjiyar A, Liu X, Shen J, Wang H (2014) Characterization of a Low Shrinkage Dental Composite Containing Bismethylene Spiroorthocarbonate Expanding Monomer. Int J Mol Sci 15:2400–2412
40. Lowe AB (2010) Thiol-ene “click” reactions and recent applications in polymer and materials synthesis. Polym Chem 1:17–36

41. Feng Y, Liang H, Yang Z, Yuan T, Luo Y, Li P, Yang Z, Zhang C (2017) A Solvent-Free and Scalable Method To Prepare Soybean-Oil-Based Polyols by Thiol–Ene Photo-Click Reaction and Biobased Polyurethanes Therefrom. ACS Sustain Chem Eng 5:7365–7373

42. Gupta RK, Ionescu M, Wan X, Radojcic D, Petrović ZS (2015) Synthesis of a Novel Limonene Based Mannich Polyol for Rigid Polyurethane Foams. J Polym Environ 23:261–268

43. STAIGER RP, WAGNER EC (1948) ISATOIC ANHYDRIDE. II. REACTIONS OF ISATOIC ANHYDRIDE WITH AMMONIA. J Org Chem 13:347–352

44. Lin-Gibson S, Bencherif S, Cooper JA, Wetzel SJ, Antonucci JM, Vogel BM, Horkay F, Washburn NR (2004) Synthesis and Characterization of PEG Dimethacrylates and Their Hydrogels. Biomacromolecules 5:1280–1287

45. Aryee ANA, van de Voort FR, Simpson BK (2009) FTIR determination of free fatty acids in fish oils intended for biodiesel production. Process Biochem 44:401–405

46. Düngen P, Schlögl R, Heumann S (2018) Non-linear thermogravimetric mass spectrometry of carbon materials providing direct speciation separation of oxygen functional groups. Carbon N Y 130:614–622

47. Johnston PK, Doyle E, Orzel RA (1988) Acrylics: A Literature Review of Thermal Decomposition Products and Toxicity. J Am Coll Toxicol 7:139–200

48. Balani, K., Verma, V., Agarwal, A. and Narayan R (2014) Physical, Thermal, and Mechanical Properties of Polymers. In: Biosurfaces. pp 329–344

49. Rahman MA, Lokupitiya HN, Ganewatta MS, Yuan L, Stefik M, Tang C (2017) Designing Block Copolymer Architectures toward Tough Bioplastics from Natural Rosin. Macromolecules 50:2069–2077

50. Khanna YP, Pearce EM (1982) Aromatic polyamides. V. Substituent effect on thermal properties. J Appl Polym Sci 27:2053–2064